Structural Engineering and Mechanics, Vol. 17, No. 1 (2004) 15-27
DOI: http://dx.doi.org/10.12989/sem.2004.17.1.015

Long-term flexural cracking of reinforced concrete members

Rajeh Z. Al-Zaid†

*Civil Engineering Department, College of Engineering, P.O. Box 800,
King Saud University, Riyadh 11421, Saudi Arabia*

(Received December 12, 2002, Accepted October 9, 2003)

Abstract. A rational and simple analytical model to predict the time varying cracking moment of reinforced concrete sections under sustained loading is developed. The modeling procedure is based on equilibrium and compatibility requirements and takes into account the interdependent effects of creep and shrinkage as well as the presence of axial loading. A parametric study is conducted in which particular consideration is given to the effects of reinforcement ratio, level of loading, and creep and shrinkage characteristics of concrete. It is concluded that the reduction in cracking moment is mainly attributed to shrinkage. The effect of shrinkage is more pronounced at low levels of sustained loading and at high reinforcement ratios. This effect is lessened by the compression steel and creep particularly when the applied moment is near the cracking moment.

Key words: cracking; creep; reinforced concrete; shrinkage; sustained loading.

1. Introduction

The serviceability performance of reinforced concrete (R.C.) members under sustained loading is complicated by the time-variant cracking moment and the interdependence of creep and shrinkage. Mechanisms of creep and shrinkage in concrete are not fully understood, and thus prediction of their effects on behavior of reinforced concrete is imprecise at best (Rosowsky *et al.* 2000). A number of models for creep coefficient and shrinkage strain have been developed in the literature, ranging in complexity from simple to highly complicated (ACI Committee 209, 1982, and Bazant and Baweja 1995).

A time-dependent analysis involves determination of strains, stresses and curvatures at critical points along the member and at different times during the life of the member. Often, a structural engineer is most interested in the final internal action after all the effects of creep and shrinkage have taken place. More over, it is well argued by many researchers that, providing the applied stress is less than 50 percent of the concrete strength, creep strains are proportional to stress (Bazant and Wittmann 1982, Gardner and Zhao 1993, and Gilbert 1988). This assumption must be made for the principle of superposition to be valid. On the other hand, shrinkage is usually expressed in terms of mean shrinkage strain defined as the average contraction of concrete over the member cross section

† Associate Professor

(Bazant and Kim 1991, Ghali 1989, and Gilbert 1999).

In most structures, shrinkage will cause a build up of tension in the uncracked tensile concrete, and the moment required to cause cracking may be substantially less than the value of the cracking moment defined by design codes (ACI 318-95 and AS 3600-1994). In some cases, shrinkage may even cause cracking under the sole effect of the member self weight (Gilbert 1999). This phenomenon is accounted for in the current literature by proposing a reduced tensile strength for concrete (Gilbert 1988).

The objective of the current research is to develop a simple, but comprehensive and rational, analytical model for prediction of the time varying cracking moment of R.C. members under sustained loading. The model is derived based on equilibrium and compatibility conditions. It takes into account the simultaneous action of creep and shrinkage and the presence of bending moment and axial loading.

2. Development of analytical model

2.1 Basic assumptions

The proposed analytical model utilizes the following basic assumptions:

1. Plane cross sections remain plane after deformation.
2. Perfect bond exists between steel layers and the surrounding concrete.
3. Both concrete and steel obey Hooke's law under service loads.
4. Creep of concrete is proportional to the elastic strains.
5. The contraction of the plane concrete section due to shrinkage is assumed uniform over the cross section.

Throughout the formulation of the proposed model, compressive forces, stresses and the corresponding deformations are assumed positive. Positive bending moments and curvatures are those which produce tension in bottom fibers of the cross section.

2.2 General considerations

Let P and M be the resultant axial force and couple at the farthest compressed fiber that are sustaineously applied to the section. The resultant couple, M, is related to the moment due to the transverse load, M_w, and the eccentric axial load, P, by:

$$M = M_w - P.e \tag{1}$$

where e is the eccentricity of P measured from the farthest compressed fiber and is considered positive if downward.

The resulting strain distributions at time t_1, when the load is initially applied, and at a later time t in the course of the member life time are schematically illustrated in Fig. 1.

2.3 Strains and stresses in concrete

The elastic and total strains at the farthest compressed fiber ($y = 0$) and at any level y of the cross-

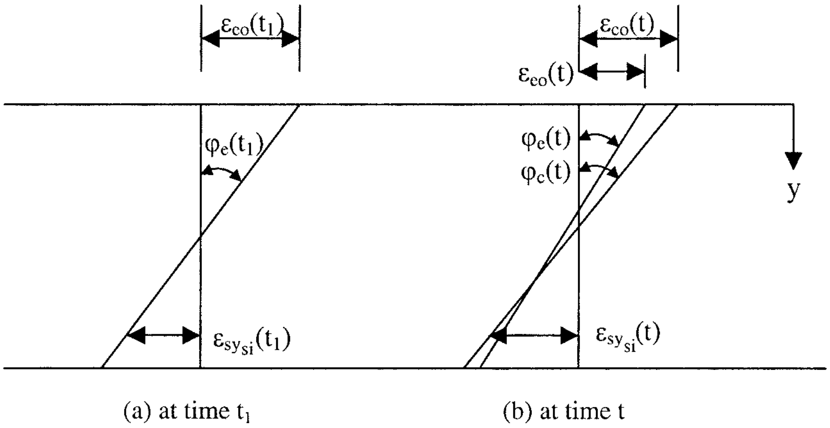

Fig. 1 Schematic illustration for strain distributions at times t_1 and t

section are denoted and expressed as follows:

$$\begin{aligned} \varepsilon_{ey}(t_1) &= \varepsilon_{eo}(t_1) - \phi_e(t_1)y \\ \varepsilon_{ey}(t) &= \varepsilon_{eo}(t) - \phi_e(t)y \\ \varepsilon_{cy}(t) &= \varepsilon_{co}(t) - \phi_c(t)y \end{aligned} \tag{2}$$

where

$\varepsilon_{ey}(t_1)$, $\varepsilon_{ey}(t)$	= elastic strains in concrete fibers located at a distance y from the farthest compressed fiber at times t_1 and t, respectively.
$\varepsilon_{eo}(t_1)$, $\varepsilon_{eo}(t)$	= elastic strains in the farthest compressed fibers (y = 0) at times t_1 and t, respectively.
$\phi_e(t_1)$, $\phi_e(t)$	= section elastic curvatures at times t_1 and t, respectively.
$\varepsilon_{cy}(t)$, $\varepsilon_{co}(t)$	= total strains at time t in concrete fibers at depth y and at the farthest compressed fiber (y = 0), respectively.
$\phi_c(t)$	= total section curvature at time t.

The terms in Eq. (2) comprise the following components:

$$\begin{aligned} \varepsilon_{eo}(t) &= \Delta\varepsilon_{eo}(t_1) + \Delta\varepsilon_{eo}(t_1, t) + \Delta\varepsilon_{eo}(t) \\ \phi_e(t) &= \Delta\phi_e(t_1) + \Delta\phi_e(t_1, t) + \Delta\phi_e(t) \\ \varepsilon_{co}(t) &= (1 + \upsilon_{1t})\Delta\varepsilon_{eo}(t_1) + (1 + \chi_{1t}\upsilon_{1t})\Delta\varepsilon_{eo}(t_1, t) + \Delta\varepsilon_{eo}(t) + \varepsilon_{sh}(t_1, t) \\ \phi_c(t) &= (1 + \upsilon_{1t})\Delta\phi_e(t_1) + (1 + \chi_{1t}\upsilon_{1t})\Delta\phi_e(t_1, t) + \Delta\phi_e(t) \end{aligned} \tag{3}$$

where υ_{lt}, χ_{1t} and $\varepsilon_{sh}(t_1, t)$ are the creep coefficient, aging coefficient and free shrinkage strain during the time interval (t_1, t), respectively. The other terms in the right hand side of Eq. (3) are as follows:

$\Delta\varepsilon_{eo}(t_1), \Delta\phi_e(t_1)$ = instantaneous strain and curvature increments due to initial loading at time t_1.

$\Delta\varepsilon_{eo}(t_1, t), \Delta\phi_e(t_1, t)$ = gradual changes in instantaneous strain and curvature due to creep and shrinkage effects during the time interval (t_1, t).

$\Delta\varepsilon_{eo}(t), \Delta\phi_e(t)$ = instantaneous strain and curvature increments due to loads applied at time t.

The stress at time t in any concrete fiber located at a distance y from the farthest compressed fiber, $f_{cy}(t)$, is given by,

$$f_{cy}(t) = E_c \cdot \varepsilon_{ey}(t) \tag{4}$$

where E_c is the modulus of elasticity of concrete which, for normal weight concrete, is evaluated by, $E_c = 4700\sqrt{f_c'}$ where f_c' is the characteristic compressive strength of concrete in MPa.

2.4 Strains and stresses in reinforcement

The strain compatibility requirement at time t implies that the strain in any steel layer at depth y_{si}, $\varepsilon_{sy_{si}}(t)$, is equal to the total strain in the surrounding concrete as given by Eq. (2). That is

$$\varepsilon_{sy_{si}}(t) = \varepsilon_{co}(t) - \phi_c(t)y_{si} \tag{5}$$

Thus, the stress in any steel layer at depth y_{si}, $f_{sy_{si}}(t)$, is given by,

$$f_{sy_{si}}(t) = E_c \cdot n_s \cdot \varepsilon_{sy_{si}}(t) \tag{6}$$

where n_s is the modular ratio E_s/E_c and E_s is the modulus of elasticity of steel.

2.5 Equilibrium equations

The preceding expressions for strains and stresses in concrete and steel (Eqs. (2)-(6)) together with the principles of mechanics of materials are employed in the force and moment equilibrium equations. The resulting expressions are rearranged to have them in the following general forms:

$$\begin{aligned} P(t) = E_c \cdot [&\{A_3 \cdot \Delta\varepsilon_{eo}(t_1) + A_2\Delta\varepsilon_{eo}(t_1, t) + A_1 \cdot \Delta\varepsilon_{eo}(t)\} \\ &-\{S_3\Delta\phi_e(t_1) + S_2\Delta\phi_e(t_1, t) + S_1\Delta\phi_e(t)\} \\ &+ n_s\varepsilon_{sh}(t_1, t)\sum A_{si}] \end{aligned} \tag{7}$$

$$\begin{aligned} M(t) = E_c \cdot [&-\{S_3\Delta\varepsilon_{eo}(t_1) + S_2\Delta\varepsilon_{eo}(t_1, t) + S_1\Delta\varepsilon_{eo}(t)\} \\ &+ \{I_3\Delta\phi_e(t_1) + I_2\Delta\phi_e(t_1, t) + I_1\Delta\phi_e(t)\} \\ &- n_s\varepsilon_{sh}(t_1, t)\sum A_{si}y_{si}] \end{aligned} \tag{8}$$

The geometric properties in Eqs. (7) and (8) are calculated for the transformed R.C. section. The first and second moments of area are taken about the farthest compressed fiber. The resulting expressions are:

$$\begin{aligned} A_1 &= A_c + (n_s - 1)\sum A_{si} \\ S_1 &= S_c + (n_s - 1)\sum A_{si} y_{si} \\ I_1 &= I_c + (n_s - 1)\sum A_{si} y_{si}^2 \end{aligned} \tag{9}$$

$$\begin{aligned} A_2 &= A_1 + (\beta - 1) n_s \sum A_{si} \\ S_2 &= S_1 + (\beta - 1) n_s \sum A_{si} y_{si} \\ I_2 &= I_1 + (\beta - 1) n_s \sum A_{si} y_{si}^2 \end{aligned} \tag{10}$$

$$\begin{aligned} A_3 &= A_1 + (\alpha - 1) n_s \sum A_{si} \\ S_3 &= S_1 + (\alpha - 1) n_s \sum A_{si} y_{si} \\ I_3 &= I_1 + (\alpha - 1) n_s \sum A_{si} y_{si}^2 \end{aligned} \tag{11}$$

where $P(t)$ and $M(t)$ are the resultant axial force and moment acting at the farthest compressed fiber of the section at time t, A_c is the area of the concrete section, S_c and I_c are the first and second moments of the area of the concrete section about the farthest compressed fiber, $\alpha = (1 + \nu_{1t})$ and $\beta = (1 + \chi_{1t}\,\nu_{1t})$.

A step-by-step solution of Eqs. (7) and (8) for the parameters of the strain distribution, $\Delta\varepsilon_{eo}$ and $\Delta\phi_e$, at times t_1 and t can be set in the following general form:

$$\begin{Bmatrix} \Delta\varepsilon_{eo} \\ \Delta\phi_e \end{Bmatrix} = \frac{1}{E_c(AI - S^2)} \begin{vmatrix} I & S \\ S & A \end{vmatrix} \begin{Bmatrix} K_f \\ K_m \end{Bmatrix} \tag{12}$$

The terms K_f and K_m in Eq. (12) are force and moment parameters, respectively. These parameters depend on the time at which Eq. (12) is solved as shown in the following sections.

3. Analysis procedure

3.1 Analysis at time t_1

At time t_1, the section at its farthest compressed fiber is instantaneously subjected to an axial load, $P(t_1)$, and a resultant bending moment, $M(t_1)$. The parameters $\Delta\varepsilon_{eo}(t_1)$ and $\Delta\phi_e(t_1)$ of the strain distribution can be obtained using Eq. (12) by setting $A = A_1$, $S = S_1$, $I = I_1$, $K_f = P(t_1)$, and $K_m = M(t_1)$.

The cracking moment at time t_1, M_{cr1}, is obtained from Eq. (12) under the condition that $K_m = M_{cr1}$ when $\Delta\varepsilon_{eo}(t_1) = f_r/E_c + \Delta\phi_e(t_1)h$ where h is the height of the section and f_r is the modulus of rupture of concrete. These substitutions in Eq. (12) lead to,

$$M_{cr1} = -f_rS_1 + (P(t_1) - f_rA_1)\left(\frac{I_1 - S_1h}{A_1h - S_1}\right) \tag{13}$$

Eq. (13) gives the resultant moment at the farthest compressed fiber of the section that causes cracking. When an axial load $P(t_1)$ exists at an eccentricity e, the portion of moment due to transverse loading that causes cracking at time t_1, M_{wcr1}, can then be obtained from Eq. (1).

3.2 Analysis at time t

During the period $t - t_1$, partially restrained shrinkage and creep gradually occur causing redistribution of strains and stresses between the concrete and steel. The section is still subjected to the sustained load $P(t_1)$ (if applicable) and the moment $M(t_1)$.

The changes in strain, $\Delta\varepsilon_{eo}(t_1, t)$, and curvature, $\Delta\phi_e(t_1, t)$, are obtained from Eq. (12) by setting $A = A_2$, $S = S_2$, $I = I_2$, and

$$K_f = P(t_1) - E_c[A_3 \cdot \Delta\varepsilon_{eo}(t_1) - S_3\Delta\phi_e(t_1) + n_s\varepsilon_{sh}(t_1, t)\sum A_{si}] \tag{14}$$

$$K_m = M(t_1) + E_c[S_3\Delta\varepsilon_{eo}(t_1) - I_3\Delta\phi_e(t_1) + n_s\varepsilon_{sh}(t_1, t)\sum A_{si}y_{si}] \tag{15}$$

The parameters $\varepsilon_{eo}(t)$ and $\phi_e(t)$ of the distribution of the total elastic strains over the concrete section are then determined by superposition as,

$$\varepsilon_{eo}(t) = \Delta\varepsilon_{eo}(t_1) + \Delta\varepsilon_{eo}(t_1, t) \tag{16}$$

$$\phi_e(t) = \Delta\phi_e(t_1) + \Delta\phi_e(t_1, t) \tag{17}$$

The maximum tensile strain in the concrete, $\varepsilon_{eh}(t)$, can then be found using Eq. (2) with $y = h$ to get,

$$\varepsilon_{eh}(t) = \varepsilon_{eo}(t) - \phi_e(t)h \tag{18}$$

Thus, the residual cracking strain, ε_{res}, is obtained from,

$$\varepsilon_{res} = \frac{f_r}{E_c} - \varepsilon_{eh}(t) \tag{19}$$

Cracking at time t will occur under the condition that,

$$\Delta\varepsilon_{eo}(t) = \varepsilon_{res} + \Delta\phi_e(t)h \tag{20}$$

where $\Delta\varepsilon_{eo}(t)$ and $\Delta\phi_e(t)$ are the strain and curvature increments due to $\Delta P(t)$ (if applicable) and the additional bending moment at the farthest compressed fiber causing cracking, ΔM_{crt}. Substituting Eq. (20) into Eq. (12) with $A = A_1$, $S = S_1$, and $I = I_1$, leads to the following solution for ΔM_{crt}:

$$\Delta M_{crt} = \left(\frac{I_1 - S_1 h}{A_1 h - S_1}\right)(\Delta P(t) - f_{res} A_1) - f_{res} \cdot S_1 \tag{21}$$

where f_{res} is the residual cracking stress = $E_c \cdot \varepsilon_{res} \le 0$.

The resultant moment at the farthest compressed fiber that causes cracking is obtained by superposition as,

$$M_{crt} = M(t_1) + \Delta M_{crt} \tag{22}$$

The portion of moment due to transverse loading that causes cracking at time t, M_{wcrt}, can then be obtained from Eq. (1).

4. Numerical example

Consider the reinforced concrete section with two layers of reinforcement and dimensions as shown in Fig. 2. The section is subjected to an axial force P = 1300 kN at mid-height and a bending moment M_w = 350 kN.m. At time t, the uniform free shrinkage, $\varepsilon_{sh}(t_1, t)$, is assumed to be 300×10^{-6} and the creep and aging coefficients, υ_{lt} and χ_{lt}, are assumed to be 3. and 0.8, respectively. The elastic moduli of concrete and steel, E_c and E_s, and the modulus of rupture of concrete, f_r, are 30 GPa, 200 GPa, and –4.4 MPa, respectively.

The preceding analysis procedure is to be used to determine the elastic strain and stress distributions at time t as well as the cracking moment of the section.

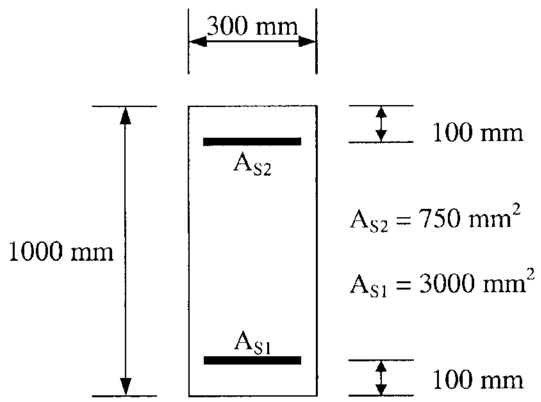

Fig. 2 Dimensions and reinforcement details of cross section used for numerical example

4.1 Preparation of model input

The equivalent force-couple system at the farthest compressed fiber is,

$$P = 1300 \text{ kN}$$
$$\text{M} = 350 - 1300 \times 0.5 = -300 \text{ kN.m}$$

The modular ratio is $n_s = \dfrac{200}{30} = 6.667$

The coefficients α and β are,

$$\alpha = 1 + v_{1t} = 4, \quad \beta = (1 + \chi_{1t} v_{1t}) = 3.4$$

The various geometric properties of the section are,

$$A_1 = 321.25 \times 10^3 \text{ mm}^2, \quad S_1 = 165.3425 \times 10^6 \text{ mm}^3, \quad I_1 = 113812.5 \times 10^6 \text{ mm}^4 \tag{9}$$

$$A_2 = 381.25 \times 10^3 \text{ mm}^2, \quad S_2 = 209.7425 \times 10^6 \text{ mm}^3, \quad I_2 = 152812.695 \times 10^6 \text{ mm}^4 \tag{10}$$

$$A_3 = 396.25 \times 10^3 \text{ mm}^2, \quad S_3 = 220.8425 \times 10^6 \text{ mm}^3, \quad I_3 = 162562.5 \times 10^6 \text{ mm}^4 \tag{11}$$

4.2 Solution at time t_1

Eqs. (12) and (13) are utilized to obtain the strain distribution parameters, $\Delta\varepsilon_{eo}(t_1)$ and $\Delta\phi_e(t_1)$, and the cracking moment, M_{cr1}. The relevant geometric properties, loading conditions, and material properties are,

$$A = A_1, \quad S = S_1, \quad I = I_1, \quad K_f = P(t_1) = 1.3 \times 10^6 \text{ N},$$
$$K_m = M(t_1) = -300 \times 10^6 \text{ N.mm, and } f_r = -4.4 \text{ MPa}$$

The resulting solutions are,

$$\Delta\varepsilon_{eo}(t_1) = 355.4 \times 10^{-6}, \quad \Delta\phi_e(t_1) = 0.4285 \times 10^{-6} \text{ mm}^{-1}$$
$$M_{cr1} = -169.3495 \text{ kN.m}, \quad M_{wcr1} = 480.65 \text{ kN.m}$$

4.3 Solution at time t

The changes in elastic strains and curvatures due to shrinkage and creep occurring during the period $(t - t_1)$ are obtained by solving Eq. (12) with the following substitutions:
$A = A_2$, $S = S_2$, $I = I_2$ and K_f and K_m are as obtained from Eqs. (14) and (15) which lead to,

$$K_f = -311.125 \times 10^3 \text{ N}$$
$$K_m = 131.51 \times 10^6 \text{ N.mm}$$

The resulting changes in strain and curvature are,

$$\Delta\varepsilon_{eo}(t_1, t) = -46.6 \times 10^{-6}, \; \Delta\phi_e(t_1, t) = -0.0353 \times 10^{-6}\ \text{mm}^{-1}$$

Thus, the changes in stresses at top and bottom of the section due to creep and shrinkage are,

$$\Delta f_{co} = -1.4\text{MPa}, \quad \Delta f_{ch} = -0.339\ \text{MPa}$$

The total elastic strain and curvature at time t are obtained using Eqs. (16) and (17) to get,

$$\varepsilon_{eo}(t) = 308.8 \times 10^{-6} \quad \text{and} \quad \phi_e(t) = 0.3932 \times 10^{-6}\ \text{mm}^{-1}$$

The corresponding stresses at top and bottom of section are 9.264 MPa and –2.532 MPa, respectively.
Thus, the residual cracking stress will be,

$$f_{res} = -4.4 + 2.532 = -1.868\ \text{MPa}$$

Eqs. (21) and (22) can then be utilized to obtain the cracking moment at time t, M_{crt}, to get,

$$M_{crt} = -189.48\ \text{kN.m}$$

which corresponds to

M_{wcrt} = 460.5 kN.m = 95.8% of the instantaneous cracking moment, M_{wcr1}.

This example was solved for strain and stress distributions by Ghali and Favre (1994) using the age-adjusted modulus of elasticity method in which shrinkage and creep were treated separately. The resulting stresses at time t were found to be,

$$f_{co} = 9.202\ \text{MPa}$$
$$f_{ch} = -2.454\ \text{MPa}$$

These stresses are almost identical to the stresses obtained by the proposed model.

5. Parametric study

A parametric study is conducted to evaluate the effects of typical design variables on the time varying cracking moment of R.C. members subjected to sustained loading. The variables considered include the reinforcement ratios of tension and compression steel, ρ and ρ', the magnitude of sustained moment M_w, and the creep and shrinkage characteristics of the concrete. The concrete compressive strength is 36 MPa and the reinforcement yield strength is 420 MPa. These properties lead to a balanced reinforcement ratio, ρ_b, of 0.0364. The shrinkage strain, $\varepsilon_{sh}(t_1, t)$, and the creep coefficient, υ_{1t}, are assumed to be in the ranges between 400 μ and 600 μ and 2 and 3, respectively. The aging coefficient χ_{lt} is taken as 0.8. The study is conducted on the typical beam and slab sections shown in Figs. 3(a) and 3(b). The developed analytical procedure is used to investigate the variation of the cracking moment (as measured by the ratio of the cracking moment at time t, M_{wcrt}, to the cracking moment at time t_1, M_{wcr1}), with the tension and compression reinforcement ratios, the level of loading, and creep and shrinkage characteristics of concrete.

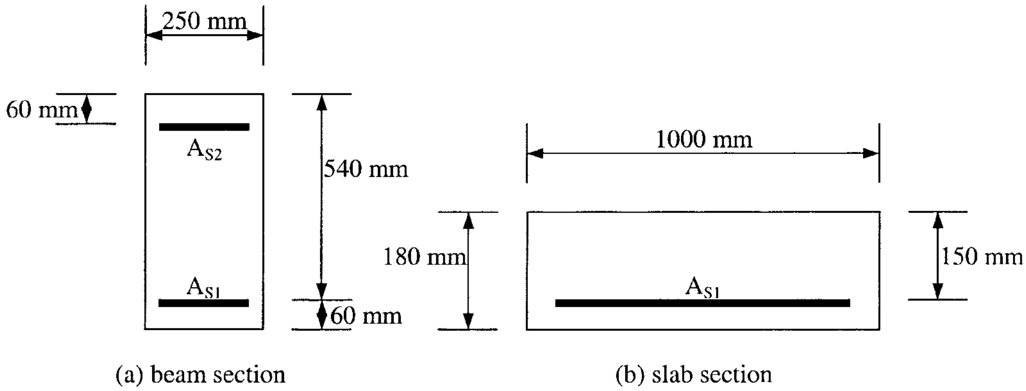

Fig. 3 Typical beam and slab sections used for the parametric study

Fig. 4 shows the variation of M_{wcrt}/M_{wcr1} with the tension reinforcement ratio, ρ/ρ_b for both the beam and slab sections at two levels of loading as measured by M_w/M_{wcr1} ratio. The plots demonstrate the detrimental effect of tension reinforcement ratio in reducing the time-dependent cracking moment. The reduction is more pronounced (50% of the instantaneous cracking moment) in sections of high reinforcement ratios and at low levels of sustained loading. The plots also indicate that time-dependent effects may lead to cracking even for sections with low reinforcement ratios if the sustained moment is near the instantaneous cracking moment.

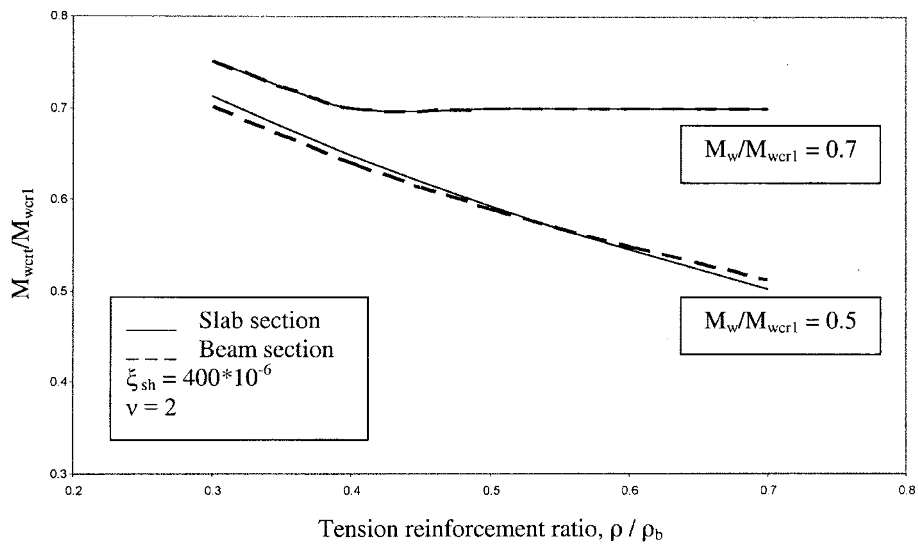

Fig. 4 Variation of long-term cracking moment with tension reinforcement ratio

Fig. 5 quantifies the effect of increased shrinkage strain on the long-term cracking moment. The plot illustrates that the shrinkage strain is the major factor affecting the long-term cracking moment magnitude. Even at low reinforcement ratios, particularly in R.C. sections subjected to low sustained moments (<50% of the instantaneous cracking moment), shrinkage may lead to significant tensile stresses in concrete to an extent that may cause cracking.

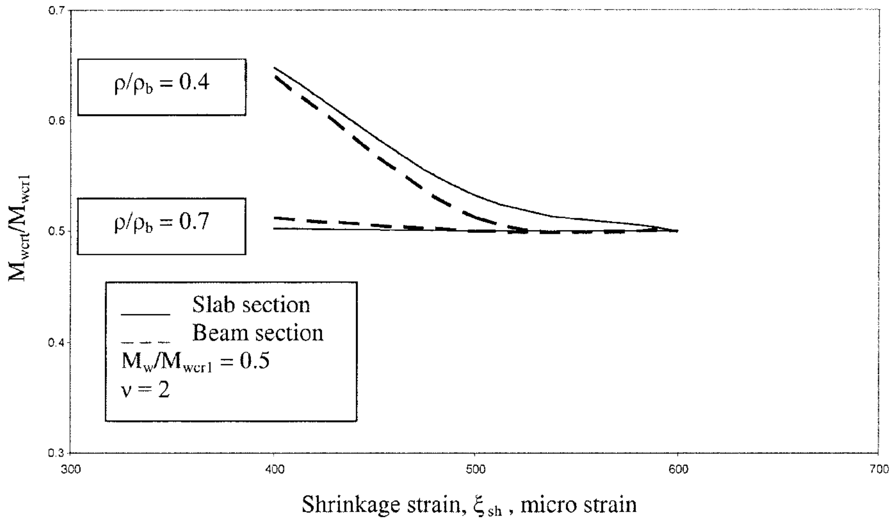

Fig. 5 Variation of long-term cracking moment with shrinkage strain

Of prime consideration is the beneficial role of creep in relieving the tensile stresses induced by shrinkage. This is clearly depicted in the plots of Fig. 6 in which the M_{wcrt}/M_{wcr1} ratio is observed to increase significantly with increased creep coefficient, υ. The rate of increase is higher in sections with high reinforcement ratios which is associated with the high shrinkage tensile stresses.

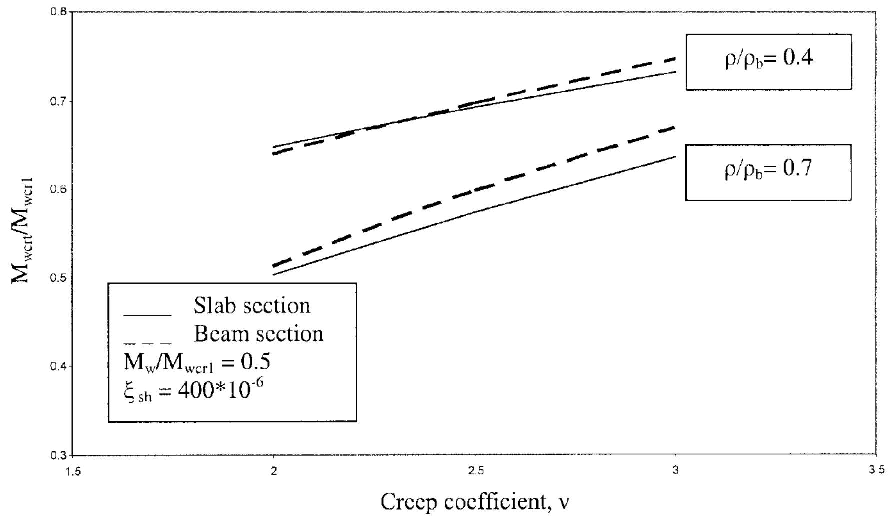

Fig. 6 Variation of long-term cracking moment with creep coefficient

The preceding trends of behavior depicted by Figs. 4, 5, and 6 are found to be almost identical for both beam and slab sections.

The effect of compression steel on improving the long-term cracking moment performance of the beam section is shown in Fig. 7. The figure reveals a moderate improvement all over the entire practical range of the compression reinforcement.

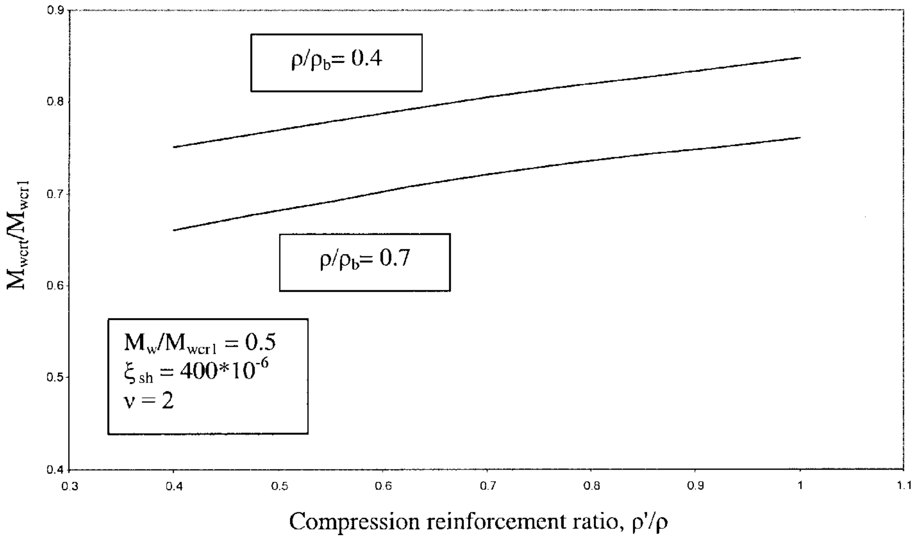

Fig. 7 Variation of long-term cracking moment with compression reinforcement ratio

6. Conclusions

The complexity in modeling the serviceability behavior of reinforced concrete under sustained loading stems from the difficulty in predicting the time-variant cracking moment and the simultaneous action of creep and shrinkage. The paper provides an analytical model, with the merit of being rationally based, to predict the time-dependent cracking moment of reinforced concrete members. The model emphasizes the concepts of equilibrium and compatibility at the specified time of analysis. It takes into account the interdependence between creep and shrinkage and the presence of axial loading and bending moment. Results of a parametric study are presented showing the effects on the long-term cracking moment of tension and compression reinforcement ratios, level of loading, and creep and shrinkage characteristics of concrete. Shrinkage and the tension reinforcement ratio are found to be the main parameters affecting the magnitude of the long-term cracking moment. The effect of shrinkage on reducing the cracking moment is more pronounced in sections with high percentages of tension reinforcement when subjected to low levels of sustained moment. Creep and compression reinforcement are observed to decrease these effects particularly when the applied moment is near the cracking moment. These trends of behavior are found to be identical for both beam and slab sections.

References

ACI Committee 318 (1995), "Building Code Requirements for Structural Concrete (ACI 318-95)", American Concrete Institute, Farmington Hills, Michigan, 351.

ACI Committee 209 (1982), "Prediction of Creep Shrinkage and Temperature Effects in Concrete Structures", American Concrete Institute, Detroit, 108.

AS 3600 (1994), *Australian Standard for Concrete Structures*, Standards, Australia, Sydney.

Bazant, Z.P. and Baweja, S. (1995), "Creep and shrinkage prediction models for analysis and design of concrete structures - Model B3", *Materials and Structures,* **28**, 357-365.

Bazant, Z.P. and Kim, J.K. (1991), "Improved prediction model for time-dependent deformations of concrete - Part 2: basic creep", *Materials and Structures*, **24**, 409-421.

Bazant, Z.P. and Wittmann, F.H. (1982), *Creep and Shrinkage in Concrete Structures*, John Wiley & Sons, New York.

Gardner, N.J. and Zhao, J.W. (1993), "Creep and shrinkage revisited", *ACI Mat. J.*, **90**(3), 236-246.

Ghali, A. (1989), "Prediction of deflection of two-way floor systems", *ACI Struct. J.*, **86**(5), 551-562.

Ghali, A. (1993), "Deflection of reinforced concrete members: A critical review", *ACI Struct. J.*, **90**(4), 364-373.

Ghali, A. and Favre, R. (1994), *Concrete Structures: Stresses and Deformations*, E & FN Spon, London, 444.

Gilbert, R.I. (1988), *Time Effects in Concrete Structures*, Elsevier Sciences Publishing Inc., Amsterdam, 321.

Gilbert, R.I. (1999), "Deflection calculation for reinforced concrete structures-why we sometimes get it wrong", *ACI Struct. J.*, **96**(6), 1027-1032.

Rosowsky, D.V., Steward, M.G. and Khor, E.H. (2000), "Early-age loading and long-term deflections of reinforced concrete beams", *ACI Struct. J.*, **97**(5), 517-524.